DEVELOPING SOIL MOISTURE MAPS IN SKELETAL SOILS USING A COSMOS ROVER

A Thesis

by

CANDICE RENEE MEDINA

Submitted to the Office of Graduate and Professional Studies of
Texas A&M University
in partial fulfillment of the requirements for the degree of

MASTER OF SCIENCE

Chair of Committee,	Haly Neely
Committee Members,	Binayak Mohanty
	Georgianne Moore
Head of Department,	David Baltensperger

May 2018

Major Subject: Soil Science

ABSTRACT

The presence of coarse fragments (rocks) can impact soil physical properties such as volumetric water content, bulk density, and plant available water. Soils containing greater than 35 percent coarse fragments by volume are considered skeletal soils. Skeletal soils can be highly sensitive to erosion, occur in ecosystems of volatile carbon fluxes, and are difficult to restore once damaged. Furthermore, desertification in skeletal soils can directly impact local inhabitants through changes in property values, tourism resources, and local agricultural economies. Due to the sensitivity of the ecosystems in which skeletal soils are found, understanding their relationship with soil moisture is crucial for best land management efforts. Although a variety of sensors can measure soil moisture, many have measurement volumes that are too small or too large to give useful information at the landscape scale. The presence of coarse fragments further complicates soil moisture measurements by increasing the spatial variability of soil properties and acting as physical barriers for in situ sensors. The cosmic-ray soil moisture observation system (COSMOS) rover is a passive, non-invasive surface soil moisture sensor with a footprint greater than 100 m. However, the COSMOS rover has yet to be calibrated in a skeletal soil. Our objective was to calibrate the COSMOS rover in a skeletal soil to assess the impact coarse fragments have on surface soil moisture sensing. COSMOS rover surveys were conducted under three soil moisture conditions. Electrical conductivity surveys were conducted to estimate the spatial distribution of coarse fragments within the COSMOS footprint for each survey. Soil samples were

taken to determine a ground measured bulk density, water content, and coarse fragment percent volume. The COSMOS measurements were then compared to the ground truth water content measurements by interpolating them over the COSMOS footprint. As expected, there was a decrease in water content as the percent volume of coarse fragment increased. COSMOS measurements responded to both changes in coarse fragment volume and changes in soil wetness with rainfall events. The COSMOS was able to accurately measure the soil water content of a skeletal soil without an additional correction factor for coarse fragment content.

DEDICATION

To my Mother and Father

My Guardian Angels

ACKNOWLEDGEMENTS

I would like to thank my committee chair, Dr. Haly Neely, and my committee members, Dr. Georgianne Moore and Dr. Binayak Mohanty, for their guidance and support throughout the course of this research. Dr. Neely's professionalism and work ethic as a woman in science will continue to set an example to me in years to come. I would also like to acknowledge Darin Desilets and Gary Womack at Hydroinnova for all of their patience and support when troubleshooting our sensor issues. A special thank you goes out to Dr. Cristine Morgan for her mentorship. She instilled in me a love for soil and always believed in my ability as a scientist. I would also like to thank Dr. Kevin McInnes for providing me with the background in soil physics I will utilize for the remainder of my professional and academic career.

Thanks goes out to the faculty and staff of the Soil and Crop Sciences Department for providing me with a positive experience. The students and faculty of the soil physics and hydropedology lab group have become a second family. Catherine Kobylinski, Sarah Vaughan, Henrique De Ros Carvalho, Gregory Rouze, Alex Garcia, Lauren Tomlin, and Dianna Bagnall are both my colleagues and friends, without which my success would not be possible.

I would like to thank my Tia Morena and Uncle Raymond, for instilling in me integrity and work values, my Auntie Cheevie and Auntie Linda for always promoting my creativity and embracing my uniqueness, and my grandparents, for showing me to take pride in everything I do. I would also like to acknowledge my cat, Lilly, for always

being the sunshine I came home to on the stressful days. Finally, I would like to thank my amazing parents and sister. Everything thing that I am and everything I do, is because of them.

CONTRIBUTORS AND FUNDING SOURCES

This work was supervised by a thesis committee consisting of Professor Haly Neely of the Department of Soil and Crop Sciences, Professor Binayak Mohanty of the Department of Biological and Agricultural Engineering, and Professor Georgianne Moore of the Department of Ecosystem Science and Management. The lattice water calculations in Chapter II were conducted by Activation Laboratories in Ancaster, Ontario, Canada. All other work conducted for the thesis was completed independently by the student. Graduate study was supported by the National Science Foundation Award No. HRD-1502335, Texas A&M University System Louis Stokes Alliance for Minority Participation (TAMUS LSAMP) Bridge to the Doctorate (BTD) Cohort XI (2015-2017) Program.

TABLE OF CONTENTS

LIST OF FIGURES

CHAPTER I

INTRODUCTION AND LITERATURE REVIEW

Intermediate scale soil moisture maps, defined as one to hundreds of kilometers, can be particularly useful for land-use planning, geological surveys, urban planning, and disaster management. Although there are a wide variety of soil moisture sensors that can be used to create these maps, they are limited by their support volume or spatial scale. Most currently available soil moisture sensors are in-situ sensors or remote sensing satellites. For instance, point measurements (< 1 m^2) such as the Theta probe have a footprint of 75 cm^3 (Delta-T Devices Ltd. 1999) while the Soil Moisture and Ocean Salinity (SMOS) satellite has a footprint of around 40 km (Collow and Robock, 2011). A major issue in scaling between point, intermediate, and large-scale platforms is the change in soil variability and its drivers at these different scales (Robinson et al., 2008). Platform linking becomes more problematic in skeletal landscapes with a high coarse fragment presence. Coarse fragments further increase soil variability and create physical barriers when using certain sensors. The existence of an intermediate scale soil moisture sensor, such as the COSMOS rover, holds the possibility of creating soil moisture maps in skeletal soils. The ability of the COSMOS rover to measure volumetric water content in skeletal landscapes has not been well studied. The objective of this study is to develop a methodology for studying soil water content at the landscape scale in skeletal soils using a COSMOS rover.

Coarse fragments are defined as particles larger than 2 mm in diameter (Brady and Weil, 2002). Soils with coarse fragment volumes of thirty-five percent or more are defined as skeletal soils and are typically deemed unsuitable for cultivation (National Resource Conservation Service, 2010). The lack of economic incentives due to its inability for agricultural use, combined with the difficulty in working in these soils due to coarse fragments hindering in-situ sensors, has greatly hindered research on the influence that coarse fragments have on soil-water dynamics (Cousin et al., 2003). These physical obstacles to sensing increase as the percentage of coarse fragment increases. For example, an investigation in potato crops found that the presence of coarse fragments can increase bulk density, macropores, and soil temperature, while decreasing total porosity and water holding capacity (Chow et al., 2007). The presence of coarse fragments can also affect the saturated hydraulic conductivity and infiltration rate of the soil, as well as increase soil erosion (Beibei et al., 2009).

Skeletal soils are most abundant in drylands, which make up roughly 40% of the earth's surface (Johnson et al., 2006). Alongside soil erosion, skeletal soils are susceptible to desertification due to deforestation and soil loss. Deforestation and soil loss, either anthropogenic or environmental, changes the physical, chemical and biological characteristics of the soil (Jiang et al., 2014). These changes often negatively impact soil health by inhibiting plant growth and altering hydrologic properties of the soil. In rocky soils these impacts happen at a faster rate and are often exacerbated. Desertification in these soils can be responsible for increases in floods, droughts, landslides, and loss of biomass, forest, vegetation cover, and biodiversity. (Jiang et al.,

2014). Most dryland inhabitants live below the poverty line and are directly affected by desertification and soil erosion. The results of both soil erosion and desertification in these areas can lead to losses of property, tourism resources, economic production, and increase the economic gap by decreasing the local work force (Jiang et al., 2014). It is estimated that $45 billion dollars a year is spent on environmental and health losses due to soil erosion in the United States alone (Pimentel et al., 2005). Skeletal soils play key roles in both human and ecological sustainability and therefore are important research areas.

High variability in the spatial distribution and lithology of coarse fragments in skeletal soils make them difficult to study at the landscape scale. To study soil water content in skeletal soils, the spatial variability of coarse fragments must be known. There has been progress on the use of proximal sensors to map the spatial distribution of coarse fragments. Two types of proximal sensors have been shown to successfully detect rocks in the soil: 1) electrical resistivity tomography (ERT) and 2) electromagnetic induction (EMI) (Doolittle et al., 2005; Samouëlian et al., 2005). Both of these sensors respond to the electrical conductivity (EC), or resistivity, of the soil. The ERT method measures the sub-surface by inserting electrodes into the soil. One electrode pair emits a direct current into the ground while another pair measures the electric potential (Samouelian et al., 2005; Amato et al., 2008). Similar to the ERT, the EMI method generates a magnetic field into the subsurface which creates eddy currents. These currents create a secondary magnetic field which is proportional to the natural electrical conductivity of the soil (McNeil, 1980; Doolittle et al., 2001). Both methods can generate maps that are

influenced by highly resistive materials such as rocks. These maps can be used to determine the influence coarse fragments have on other soil moisture technology (McNeill, 1980). Although these two methods can be used over large areas, it is difficult to obtain land-scape and regional-scale maps using these techniques because of the time needed to cover such a large area.

Proximal sensing techniques may respond to multiple soil properties. These properties change over different soil types and spatial scales. Identifying which soil properties are driving the response of the sensors makes it challenging to interpret the data. Another problem can arise in highly responsive soils, where the EMI method may not be able to generate the second magnetic field if the measurement range is exceeded. Furthermore, common EMI devices such as the EM38-MK2 (Geonics, Mississauga, Ontario, Canada) with a measurement accuracy of +/- 5% at 30 mS m^{-1}, can have significant error in low conductivity soils.

At the large (>10 km) scale, satellite remote sensing approaches are commonly used to estimate soil water content. Remote sensing techniques allow for continuous, nonobtrusive monitoring for climate, water dynamics, and agricultural purposes worldwide. This is especially useful in inaccessible regions where field expeditions are not possible. However, despite the global mapping and measurement capabilities of large scale remote sensing, it is limited in remote areas where calibration and validation are difficult to obtain. Some studies have evaluated the limitation of remote sensing techniques in rocky (skeletal) soils (Sano, 1998; Walker et al., 2009; Ye et al., 2009). In 1998, a study was conducted to evaluate the European remote sensing satellite ERS1-

SAR radar to estimate soil moisture on rocky, rough surfaces. The study found that although the SAR data was a good estimate for surface roughness, it performed poorly in measuring soil moisture without removing vegetation cover and surface roughness (Sano et al., 1998). The most direct study was done by Walker et al. (2009), where the effect rock cover fraction had on L-band retrieval influenced the accuracy of soil moisture measurements for SMOS. The study found that, when rocks were omitted from the retrieval algorithm, SMOS overestimated soil moisture in drier conditions and underestimated in wet conditions. The maximum error was 0.04 $m^3 m^{-3}$ in bare soil and 0.10 $m^3 m^{-3}$ in wet soil (Ye et al., 2009). Walker et al. (2009) concluded that rock cover can have a significant impact on soil moisture measurements and that further research should focus on understanding this influence and finding use of its application.

The cosmic-ray soil moisture observing system (COSMOS) (Hydroinnova, LLC, Albuquerque, N. M., USA) is an intermediate-scale (100 m), passive neutron surface soil moisture sensor. It relies on incoming cosmic-ray radiation from the atmosphere to measure the amount of water in the soil. Cosmic ray protons react with the earth's atmosphere to produce secondary fast neutrons. These secondary neutrons collide with and are thermalized by hydrogen. The more hydrogen that is contained in the soil (found primarily in water), the more neutrons are being thermalized and this lowers the number of fast neutrons detected above ground. Soil moisture can be calculated inversely by measuring the fast neutron intensity (Zreda et al., 2008). Other pools of hydrogen exist, such as lattice water (water bound to the soil above drying at 105°C) and vegetation biomass, which can be corrected for in the calibration equation for the

COSMOS (Desilets et al., 2010). Other factors affecting incoming neutron intensities also need to be normalized including atmospheric pressure and solar activity.

There are now over 200 stationary COSMOS probes across the globe. Recent publications regarding COSMOS have focused on a range of applications including evaluating evaporation model estimates and assimilation of neutron counts for irrigation scheduling (Han et al., 2016; Jana et al., 2016). Another use of COSMOS probes is in evaluating remote sensing technologies. Renzullo et al. (2014) used the COSMOS probes to evaluate the Advanced Microwave Scanning Radiometer-EOS (AMSR-E) and The Advanced Scatterometer (ASCAT) satellite data to make an operational water balance modelling system. In 2015, COSMOS probes were used to assess soil moisture products from two AMSR2 sensors, and in 2016 were compared to SMOS and GLDA satellite data to evaluate their accuracy (Kim et al., 2015; Kedzior et al., 2016). Other publications assess COSMOS accuracy in high, cold ecosystems and the translation of COSMOS output into sub-kilometer soil moisture profiles to make subsoil moisture maps (Zhu et al., 2016; Rosolem et al., 2014). Although COSMOS probes have proven valuable in evaluating surface soil moisture measurements from remote sensors, testing the accuracy of the probes in more extreme environments is still underway. Currently, there has been no research on any limitations the COSMOS rover may have in skeletal soils which could influence neutron intensity counts, and therefore, volumetric water content readings (Dong et al., 2014). We expect coarse fragments to have a significant influence on soil water content as well as the COSMOS rover counts.

There are many challenges in combining data from different spatial scales, as well as predicting spatial patterns of soil properties in unmeasured areas. With the use of digital soil mapping techniques, we can build spatial maps based on other landscape properties. Digital soil maps are quantitative predictive models, using both field and statistical applications to infer and predict properties and patterns in the soil at varying spatial and temporal dimensions (Boettinger et al., 2010). Spatial statistics are used to relate soil properties to covariates in the environment. Digital soil mapping applies an inference system, which uses known data to predict unknown variables through pedotransfer functions. The most popular inference methods are regressions, classification/discrimination analysis, and the tree method. Examples of these methods are correlating plant height to water holding capacity or linking an increase in gastric cancer risk to heavy metal pollutants. The SCORPAN (soil, climate, organisms, topography, parent material, age, space) approach is a key concept behind digital soil mapping, making it possible to use various quantitative datasets to predict the outcome of another variable (McBratney et al., 2003).

Remote sensing techniques, as well as smaller-scale projects, have been used to develop digital soil maps. We predict that it is possible to up-scale between point measurements and proximal sensors to create digital soil maps of coarse fragments at the landscape scale. These digital maps are capable of correcting remote sensing platforms that measure soil water dynamics. The COSMOS rover can also be used to create these intermediate scale maps to further aid in validating both digital soil maps and remote sensing platforms. This study investigated the accuracy of soil moisture measurements

by a COSMOS rover conducted in skeletal soils in Marfa, Texas. Multiple COSMOS surveys were conducted at different soil moisture conditions. Maps of the spatial distribution of coarse fragments were developed using the EM38-MK2 and point measurement locations were selected based on these maps. This map was then used to assess and correct the COSMOS measured data. The overall objective of this study was to develop a methodology for studying soil water content at the landscape scale in skeletal soils. This was accomplished using the following objectives:

1) Investigate the accuracy of soil moisture measurements by a COSMOS rover in skeletal soils and;
2) Develop methodology for mapping soil moisture with a COSMOS rover using digital soil mapping techniques in skeletal soils.

CHAPTER II

DEVELOPING SOIL MOISTURE MAPS IN A SKELETAL SOIL WITH A COSMOS ROVER

2.1 Introduction

Soils containing coarse fragments, soil particles greater than 2 mm in size (Brady and Weil, 2002), are diverse and found across the globe (Miller and Guthrie, 1984; Ma and Shao, 2008). Soils containing 35 percent or more coarse fragments are defined as skeletal soils (FAO, 2006; Soil Survey Staff, 2010). Because skeletal soils can be found across all soil types and ecoregions, there is no definitive understanding on their role in soil-water dynamics (Miller and Guthrie, 1984). Skeletal soils can be highly sensitive to erosion (Poesen and Lavee, 1995), can occur in ecosystems with volatile carbon fluxes (Throops et al., 2012), and are difficult to restore once damaged (Jiang et al., 2014). The results of both soil erosion and desertification in these areas can lead to losses of property, tourism resources, economic production, and increase the economic gap by decreasing the local work force (Jiang et al., 2014). In contrast, the presence of coarse fragments in arid and semi-arid regions can aid in the productivity and sustainability of the ecoregion by influencing runoff frequency and magnitude and soil desalinization (Yair and Shachak, 1987).

This investigation focused on dryland skeletal soils. Drylands are regions defined by their scarcity of water, which is the limiting factor for primary production and nutrient cycling (Millenium Ecosystem Assessment, 2005). Drylands account over

roughly 40% of the earth's surface (Johnson et al., 2006) and are at a higher sensitivity to environmental changes due to their low water holding capacity and potentially high erodibility (Beibei et al., 2009). The high susceptibility to erosion puts the overall ecosystem health at risk. Alongside soil erosion, drylands are susceptible to desertification due to deforestation and soil loss. Deforestation and soil loss, either anthropogenic or environmental, changes the physical, chemical and biological characteristics of the soil (Jiang et al., 2014). These changes often negatively impact soil health by inhibiting plant growth and altering hydrologic properties of the soil. In rocky soils these impacts happen at a faster rate and are often exacerbated. Desertification can be responsible for increases in floods, droughts, landslides, and loss of vegetation cover and biodiversity (Jiang et al., 2014). Due to the sensitivity of the ecosystems within which skeletal soils are found, understanding their relationship with soil moisture dynamics is crucial for conservation and best land management practices.

Although there are a wide variety of sensors that can be used to measure soil moisture, many have measurement volumes that are too small or too large to give useful information at the landscape scale. Most currently available soil moisture sensors are either point scale in-situ sensors (<1 m) or large scale (>10 km) remote sensing satellites. Creating moisture maps at the landscape scale (10-100 m resolution) from either sensor type proves to be problematic due to the different sensor support volume and spatial resolution. The presence of coarse fragments increases this difficulty by increasing the spatial variability of soil properties as well as acting as physical barriers when using in situ sensors (Robinson et al., 2008). However, including knowledge of

coarse fragments is crucial because coarse fragment content can be highly spatially variable across landscapes (Flint and Childs, 1984). A study by Cousin et al. (2003) found when rock fragments are neglected, the available water content of the soil can be overestimated by up to 39%, while including rock fragments but neglecting their hydraulic properties can lead to underestimations by 34%. Subsurface rock fragments have been documented to affect infiltration rate, soil structure, porosity, and permeability (Poesen and Lavee, 1994).

Electromagnetic induction (EMI), a non-invasive, proximal sensor, has been shown to detect the variability in coarse fragment content in rocky (skeletal) soils (McNeil, 1980). Because the EMI method relies on generating a magnetic field in the soil and measuring the bulk apparent electrical conductivity (EC_a) of the soil (McNeil, 1980; Doolittle et al., 2001), the strength of the signal is directly influenced by highly resistive materials such as rock minerals (McNeil, 1980). Although this method can be used at the landscape scale (100-m scale), it is very difficult to obtain landscape scale maps using this technique because of its relatively small footprint (approximately 1 m^2). Electromagnetic induction is also limited by its cumulative response to multiple soil properties including soil salinity, clay content, and soil water content (McBratney et al., 2005). This problem is increased further for highly resistive soils where it is difficult to create the secondary magnetic field (McNeil, 1980).

The cosmic-ray soil moisture observation system (COSMOS, Hydroinnova LLC Albuquerque, New Mexico) rover is an intermediate-scale, passive neutron surface soil moisture sensor. Cosmic-ray particles from sources in space enter the atmosphere,

collide with atmospheric nuclei and produce secondary neutrons. These neutrons interact with hydrogen to produce thermalized neutrons. Because hydrogen in the soil is found predominantly in water, the neutron count above the surface and can be inversely related to the amount of water in the soil (Zreda et al., 2008). Other pools of hydrogen exist outside the soil profile. These include lattice water, vegetation cover, and atmospheric water vapor. Alongside this, neutron intensity fluctuates with temperature and location (Desilets and Zreda, 2003). Spatially, neutron intensity is at its minimum and increases horizontally from the geomagnetic equator, and vertically towards the poles. Intensity also decreases with an additional 100 hPa pressure. This is due to the increase interaction between the fast neutrons and the nuclei in the atmosphere (Desilets and Zreda, 2003; Desilets et al., 2006). Neutron intensity is primarily related to solar activity and barometric pressure. Stronger solar activity decreases the number of protons entering our atmosphere, which in turn reduces the amount of fast cosmic-ray neutrons produced. Changes in atmospheric pressure, which changes with weather conditions, alters the amount of atmospheric shielding of cosmic-rays (Desilets et al., 2006). At higher elevations, there are fewer air molecules, therefore as elevation increases atmospheric pressure decreases.

Contrary to in-situ sensors, the COSMOS rover is non-invasive and has a measurement footprint of over 100 m. This instrument has potential to provide soil moisture information at the landscape scale but has not been validated on a soil with coarse fragments.

Currently, there has been no published research on soil moisture maps as measured by a COSMOS rover in skeletal soils. The objectives of this study were to 1) investigate the accuracy of soil moisture measurements by a COSMOS rover in skeletal soils and 2) develop a methodology for continued measurement of. We will use EMI and soil sampling to calibrate the COSMOS rover using multiple surveys under different soil moisture conditions. We expect coarse fragments to have a significant influence on soil water content as well as the measurements from the COSMOS rover.

2.2 Methods

Calibrating a surface soil moisture sensor in a skeletal soil has a distinctive set of challenges including needing large soil samples (> 18 L volume) and the increased spatial heterogeneity at the 10-m scale compared to soils without coarse fragments. To address this, we used a proximal soil sensor, the EM38-MK2, to map the spatial variability of coarse fragments within the COSMOS footprint and sample locations and to provide information for spatially interpolating samples across the COSMOS footprint. The general field procedure for calibrating the COSMOS was: 1) conduct a landscape-scale survey covering roughly 2,000 ha, 2) select contrasting areas in the survey using k-means classification and conduct an EM38-MK2 survey of the COSMOS footprint, and 3) use k-means classification of the temperature-corrected bulk apparent electrical conductivity (EC_{25}) to select three locations for soil sampling, 4) collect large volume surface soil samples for soil moisture and coarse fragment volume, 5) Upscale the ground measured samples to the COSMOS footprint using ordinary kriging interpolation, 6) convert COSMOS raw neutron counts to volumetric water content using

the universal calibration equation and ground measured bulk density and finally 6) compare the spatial mean ground measurements to the COSMOS estimates soil water content to determine if COSMOS is accurately estimating soil moisture in a texas skeletal soil.

2.2.1 Site Description

Research was conducted at the Mimms Unit of the Dixon Water Foundation, a 4,500-ha ranch, on the northwest edge of Marfa, Texas, in Presidio County on the eastern portion of the Chihuahuan Desert (Figure 2-1). The Mimms Unit is a working cattle ranch, whose primary mission it to promote healthy watersheds by practicing economical conservation practices. The ranch receives around 402 mm annually, with the highest months of precipitation being between July and September. The main vegetation consists of creosote bush, lechuguilla, prickly pear, yucca, agave, stool, and ocotillo. The most common grasses on the ranch and throughout this desert region are black grama and toposa grass. Elevation on the ranch is variable with a significant number of rock outcrops, and ranges between 1400 and 1600 m (Fishburn and Carswell, 2017). The ranch is located on the edge of the Davis Mountains landform, originating roughly 35 million years ago when volcanic activity was high in western North America. The mountains and outcrops in this area are composed of magma that erupted from both the Paisano Volcano and the Buckhorn Caldera. The landscape in the ranch shows evidence of this geomorphology, with rugged plateaus having short grasses, and high sloped outcrops derived from colluvium and Aeolian deposits.

Figure 2-1: Aerial image of the Mimms Unit Ranch owned by the Dixon Water Foundation in Marfa, TX. The two predominant soil types observed were the chianti-boracho-berend association (CND) and marfa clay loam (MCA). The green outline is the border of the ranch. Aerial image from Esri World imagery (ESRI, 2012).

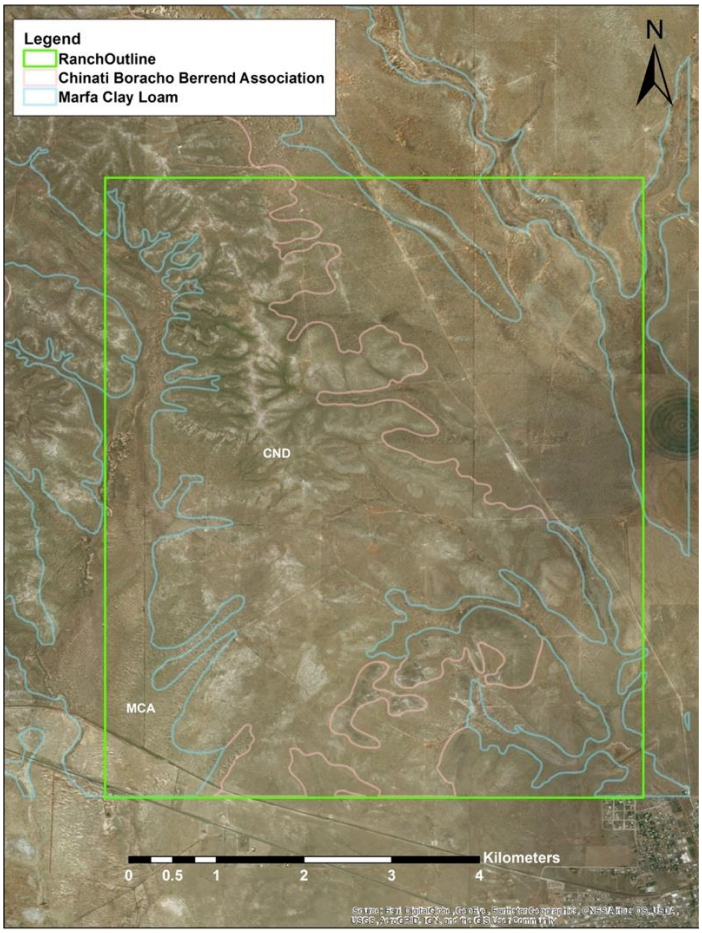

There are two dominant soil types on the ranch. The first is a Chinati-Boracho-Berrend association (loamy-skeletal, mixed, superactive, thermic, shallow petrocalcic Paleustolls) formed from gravelly alluvium derived from igneous rock. A typical pedon is a very gravelly loam with a clay content of 18-35% and slopes from 1-15%. Roughly 30% is subgrounded gravel, 20% cobbles and 10% stones. The second major soil is a Marfa clay

loam (Fine, mixed, superactive, thermic, pachic, Argiustoll) formed from loamey and clayey alluvium derived from tascotal tuffaceous sandstone, perdiz igneous conglomerate, and eolian material. It is usually found on valley floors in the area. Rocks found in the area are cinnabar, granite, opal, and more commonly, basalt. Figure 2-1 shows an aerial image of the Mimms Unit ranch with an outline of the two dominant soil types. Figure 2-2 shows the stark contrast on the surface at two locations with the different soil types and the general land formation found on the ranch The USGS mapped the ranch as having alluvium and perdiz conglomerate from the tertiary and quaternary period, shed from northeast.

Figure 2-2: Surface images of the dominant soil types and box diagram of typical land formations on the ranch. **A)** Surface images of the Marfa clay loam soil. No visible surface fragments can be seen. Dominant vegetation on these areas of the ranch were grasses. **B)** Surface images of the shallow Chianti-Boracho-Berrend association soil. Visible coarse fragments can be seen on the surface. **C)** Box diagram of the general land formations on the ranch. Aerial image from Esri World imagery (ESRI, 2012).

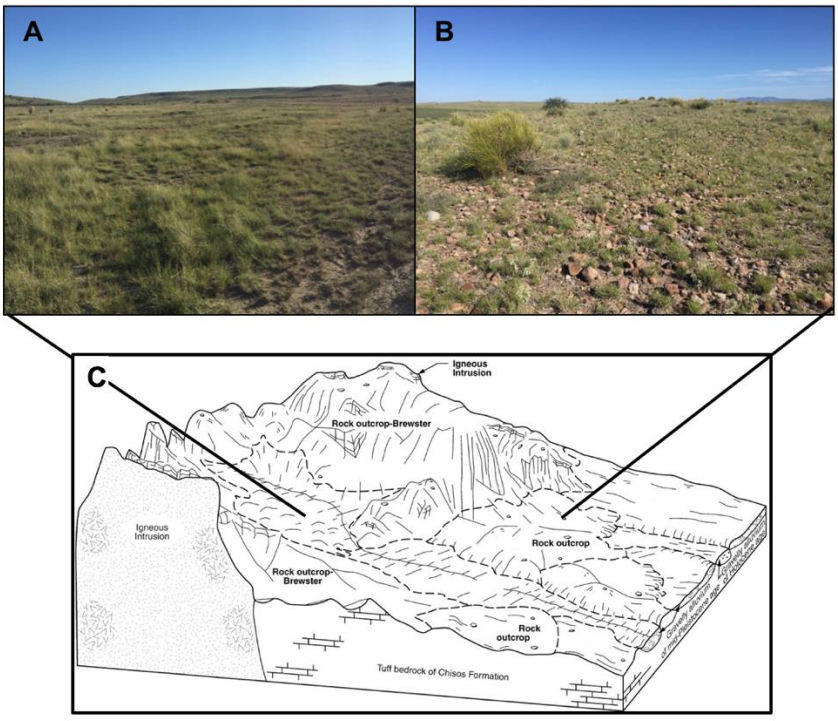

2.2.2 COSMOS Rover Surveys

Soil moisture surveys were conducted using a COSMOS rover on the Mimms Unit ranch in Marfa, Texas, on August 4th 2016, August 16th 2016, and January 7th 2017. The August 4th survey was taken 72 hours following a minor rain event where the ranch received roughly 17 mm of rain**.** The August 16th survey was taken within 48 hours of a major rain event, where the ranch received over 43 mm of rain. The January 9th survey was taken during dry conditions, where the ranch experienced no rainfall for 51 days

leading up to the survey. The COSMOS rover and data logger were secured and driven in a 2016 Toyota Highlander, averaging 16 kmph for each survey. GPS coordinates were collected with a BR-355S4 GPS receiver (US GlobalSat, Inc., California, USA), and both air temperature and relative humidity were measured using a Campbell Scientific CS215-L temperature and relative humidity probe (Campbell Scientific, Inc., Utah, USA) throughout each survey. The COSMOS rover was driven over as much of the ranch as was permitted by pasture access and drivability. No established route was followed. Although the ranch has relatively consistent vegetation cover, different sizes of coarse fragments can be observed; the higher slopes (hillslopes) were seen to have greater amount of rocks on the surface, while the lower elevated plains of the ranch appeared to have few or no surface fragments. The COSMOS rover was driven over visually contrasting areas to ensure varying percentages and size distribution of coarse fragments were surveyed.

2.2.3 Bulk Apparent Electrical Conductivity Surveys

Two COSMOS points were chosen using k-means classification, which clusters *k* observations into *n* number of clusters with the nearest mean (R Core Team, 2013) for each COSMOS survey. To conduct EM38-MK2 (Geonics Ltd., Ontario, Canada) surveys, "high" and "low" neutron count locations were chosen, where areas of low/high soil water contents were expected to be observed. Both the 0.5 and 1 m coil spacing in the vertical dipole mode was used, and soil temperature was recorded at the beginning of each survey 5 cm below the surface. There was a total of six electrical conductivity surveys, one at each chosen COSMOS footprint, over the three survey expeditions. We

corrected for temperature differences by using the equation developed by Sheets and Hendrickx (1995):

$$EC_{25} = EC_a * [0.4470 + 1.4034e^{\frac{T}{26.815}} \quad (1)$$

Where EC_{25} is the standardized electrical conductivity to 25°C, and T is the temperature of the soil in degrees C. The EM38-MK2 was walked in a circular pattern starting at the COSMOS coordinate out to 200 m in all directions. Distance between transects began at 5 m spacing and changed to 25 m spacing after a 50 m distance, and 50m spacing after a 100 m distance from the COSMOS rover. The COSMOS rover has been reported to have an approximately 600-m diameter footprint; however, a more conservative area of interest was chosen to ensure the EMI data would overlap with the area that contributed most to the fast neutron counts measured by the COSMOS.

2.2.4 Soil Samples

A map of each EM38-MK2 survey was created and stratified random sampling using k-means clustering with three clusters was used (Figure 2-3) to select soil sampling locations.

Figure 2-3: Map of temperature corrected apparent electrical conductivity at the COSMOS high (neutron) site on August 4th, 2016. The white x's represent chosen soil sample locations. Aerial image from Esri World imagery (ESRI, 2012).

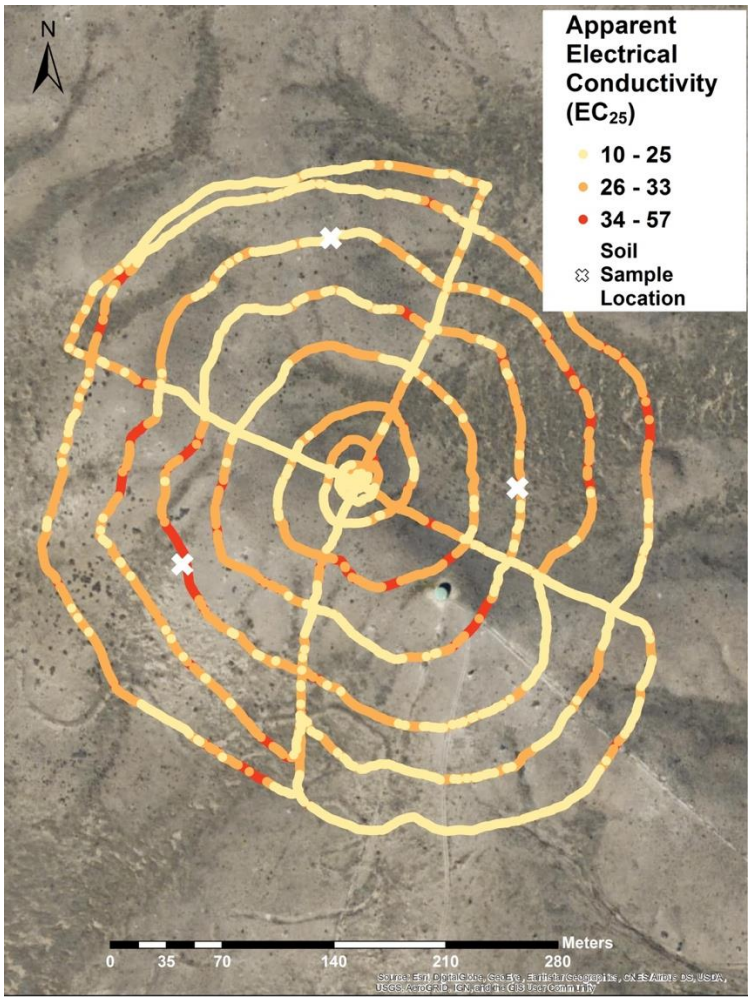

Soil samples were collected to determine bulk density, coarse fragment mass and volume, and gravimetric and volumetric water content. *In situ* bulk density was measured using a volume replacement method. The volume of soil samples was chosen based on the ASTM standard (ASTM, 2015), which states that as particle size increases,

the sample size must increase also. Due to the varying size of the particles being collected (some greater than 50.8 mm in diameter) the sample size will be equal to or greater than 25 kg, or approximately the size of a 5-gallon (19 L) bucket. One sample was taken randomly within each k-means cluster, totaling three samples at each COSMOS footprint. Samples were taken to a depth of 30 cm and weighed on site with a portable balance. This depth was chosen for several reasons, the first being that the measurement depth of the COSMOS increases as the moisture condition of the soil decreases (Franz et al., 2012b). Given the soil has a small water holding capacity, the soil was assumed to be dry enough that the COSMOS could effectively measure the first 30 cm of soil moisture. This falls in line with typical calibrations between 0- 30 cm (Franz et al., 2012b). Another reason this depth was chosen was due to the measurement depth of the EM38-MK2 sensor. The EM38-MK2 has a measurement depth of 0.5 m, or 50cm. Due to the abundance of resistive rocks and shallow depth to bedrock, the sensor was presumed to only be measuring the top 30 cm of soil. These assumptions allowed us to reconcile the two sensors to a similar measurement depth.

Once mass was measured, the hole was filled and leveled with sand of a known bulk density. The mass of the sand used was measured to calculate the soil volume. Subsamples of each bulk sample were collected to measure gravimetric water content, for calibration of the COSMOS data (described below). There was a total of 18 soil samples between the three separate COSMOS survey dates.

Coarse fragment percentage was measured by separating the particles from the finer fraction via wet sieving. Each bulk sample was soaked in a chemical dispersant

(sodium hexametaphosphate) solution for 24 hours. Each bulk sample's coarse fragments were sieved through four different grades of sieve (75 mm, 22.4 mm, 4.75 mm, and 2 mm). The coarse fragment volume from each sieve class was measured by volume displacement.

To obtain a mean water content for the COSMOS footprint, first the k-means clusters of EC_{25} data were spatially interpolated over the footprint using inverse distance weighting. Then each cluster was assigned a measured water content from the soil samples. Instead of taking a simple mean water content of the spatially-interpolated map, values closer to the COSMOS rover were weighted higher than values further away based on the weighted function in Schron et al., 2017. The weights and the distance from the COSMOS center were as follows: 40% weight at 10 m, 25% at 25 m, 20% at 50 m, 10% at 100 m, and 5% at 200 m. This spatially-weighted mean soil water content was then compared to the COSMOS measured water content.

2.2.5 COSMOS Data Analysis

2.2.5.1 Correcting Neutron Counts

Before using the universal calibration equation, the raw neutron counts were corrected for atmospheric pressure, atmospheric water vapor, and high-energy neutron intensity (Zreda et al., 2012). The formula to correct the raw neutron counts is:

$$N = \frac{N_{raw} * CP * CWV}{CI * CS} \tag{2}$$

where N is the corrected neutron counts, N_{raw} is the raw neutron counts collected by the instrument, CP is the atmospheric pressure correction factor, CWV is the atmospheric

water vapor correction factor, *CI* is the high-energy neutron intensity correction factor, and *CS* is the scaling factor for geomagnetic latitude (Zreda et al., 2012).

The correction factor *CP* is calculated using the following formula:

$$CP = e^{\frac{(P-P_0)}{\lambda}} \tag{3}$$

where *P* is the barometric pressure (mb) over the counting interval collected by the rover, P_0 is the reference pressure (mb) at the site. This was determined by using the COSMOS utility calculator on the COSMOS website (http://cosmos.hwr.arizona.edu/Util/calculator.php) based on the equations from Desilets and Zreda (2003) and uses the reference location of the ranch. Lambda (γ) is the natural neutron attenuation length in air of 130 g cm^{-2}, which is a constant over the continental United States (Desilets and Zreda, 2003).

In order to determine the atmospheric water vapor during the time of survey, the saturated vapor pressure, actual vapor pressure and absolute humidity are needed. The saturated vapor pressure can be calculated by:

$$es_0 = 611.2 * e^{\frac{(17.67*T)}{(243.5+T)}} \tag{4}$$

where es_0 is the saturated vapor pressure (Pa) and *T* is the air temperature (^{O}C). Once the saturated vapor pressure is calculated, the actual vapor pressure at the surface can be calculated with the following:

$$e_0 = \frac{H_r}{100} * es_0$$

(5)

where e_0 is the actual vapor pressure at the surface (Pa) and H_r is the relative humidity (%). The absolute humidity is calculated by using the equation:

$$\rho_v = \frac{e_0}{R_{vap} * (T + 273.15)} * 1000$$

(6)

where ρ_v is the absolute humidity and R_{vap} is the gas constant for water vapor, 461.51(kg mol^{-1}). T is the air temperature (^{O}C). The water vapor correction factor is:

$$CWV = 1 + (.0054 * \rho_v' - {\rho_v}^0)$$

(7)

where CWV is the water vapor correction factor, ρ_v' is the absolute humidity (g m^{-3}) at the time of the survey, and ρ_v^0 is the reference absolute humidity (g m^{-3}) (Rosolem et al., 2013).

The high energy neutron intensity correction factor is determined by the following:

$$CI = \frac{{N_H}^i(t)}{{N_H}^0}$$

(8)

where CI is the high energy neutron intensity correction factor, N_H^i is the current high energy neutron intensity, and N_H^0 is the reference high energy neutron intensity, determined by using the intensity calculator found on http://cosmos.hwr.arizona.edu/Util/computeIntens.php that was derived from Zreda et al., 2012. The scaling factor correction is determined by using the utility calculator as

well. The chosen latitude and longitude used for the utility calculator were 30.35115° and -104.06709°, at the ranch headquarters. The reference elevation was 1460 m. Based on these values, the cutoff rigidity was 5.14 GV and the scaling factor was 1.78. For our study, we calculated water contents when the scaling factor was fixed and allowed to change with elevation, which will be discussed later. The overall elevation range for the COSMOS surveys was between 1460 m and 1600 m, and the scaling factor range was between 1.7 and 1.98.

2.2.5.2 Converting Neutron Counts to Volumetric Water Content

Once the neutron counts were corrected for pressure, water vapor, and neutron intensity, the universal equation can be used to convert the corrected counts to soil volumetric water content:

$$\theta_v = \left(\frac{\alpha_0}{\frac{N'}{N_0} - \alpha_1} - \alpha_2 - \omega_{\text{lat}} \right) \rho_b \tag{9}$$

Where α_0 is 0.0808, α_1 is 0.372, α_2 is 0.115, and are universal parameters of the instrument (Desilets et al., 2010). Additionally, θ_v is volumetric water content, ρ_b is bulk density (g cm^{-3}), w_{lat} is lattice water (g g^{-1}), N' is corrected neutron counts (cpm), and N_0 is the neutron count under dry soil conditions (cpm)= and if often treated as a fitting parameter.

The reference COSMOS survey used for calibration was on August 4th, 2016. All reference conditions needed for correcting the neutron counts is based on this survey.

The bulk density calculated from the 6 ground measured samples (1.6 g cm^{-3}) was used in the calibration equation. This bulk density is representative of the total sample, including coarse fragments. The fitting parameter for calibration, N_0, was determined by fitting the soil volumetric water content of the COSMOS to spatial mean ground measured water contents taken on August 4th, 2016 on a 1:1 calibration line. Each COSMOS survey thereafter used the N_0 parameter determined for the August 4th that survey. The correction factors for atmospheric pressure, neutron activity and atmospheric water vapor pressure were corrected for each survey. Subsamples were sent to Activation Laboratories (Ontario, Canada) to determine the amount of crystalline water in the samples, also known as lattice water. The results concluded that less than 3% of the soils contained lattice water by volume. This percentage was consistent across the research site and was included in the calibration.

2.3 Results

2.3.1 Soil Samples

Coarse fragment volume ranged from 2 mm in diameter to greater than 75 mm, with 40% of fragments between 4.75 to 22.4 mm (Figure 2-4). Coarse fragment percent volume in the collected samples ranged from 0.05 m^3 m^{-3} to 0.67 m^3 m^{-3}, and were consistent to their COSMOS location, i.e., higher volumes at the high-count sites and lower volumes at the low-count sites. Volumetric water contents ranged from 0.06 m^3 m^{-3} to 0.33 m^3 m^{-3} for the COSMOS survey below field capacity, 0.12 m^3 m^{-3} to 0.32 m^3 m^{-3} at field capacity, and 0.03 m^3 m^{-3} to 0.18 m^3 m^{-3} for the dry survey. The spatial average for the COSMOS high site locations from wettest to driest survey was 0.21 m^3 m^{-3}, 0.08

m^3 m^{-3} and 0.05 m^3 m^{-3}. The spatial average for the COSMOS low site locations from wettest to driest survey was 0.24 m^3 m^{-3}, 0.12 m^3 m^{-3} and 0.10 m^3 m^{-3}.

Figure 2-4: Coarse fragment size distribution found across all survey dates. Size distributions were based on standard sieve sizes.

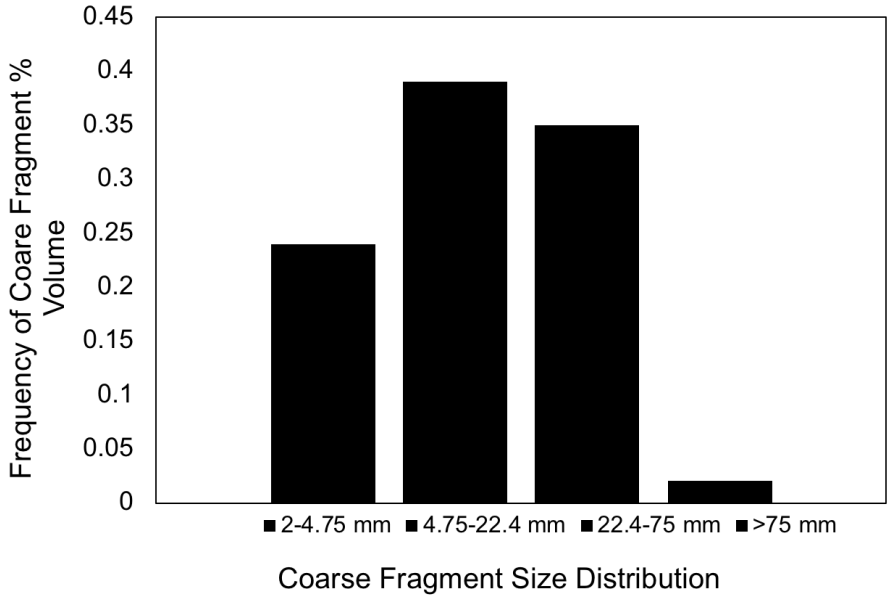

2.3.2 Electrical Conductivity Surveys

The temperature corrected EC_{25} values observed across all surveys was between 4.23 and 61.81 mS m^{-1}, which falls within the range of conductance values for weathered volcanic rocks, carbonate rocks, and unconsolidated sediments (Palacky, 1987). The EC_{25} values in this study appeared to not have any consistent relationship with changes in coarse fragment mass and volume (Figure 2-5 and 2-6). This was not surprising, as previous studies have shown erratic fluctuations of electrical conductivity when rock

fragments are on the surface or for very shallow soils containing rocks (McNeill, 1980; Doolitte et al., 2013). Nonetheless, the EM38-MK2 surveys did respond to increases in soil water content between each survey (e.g. the dry survey EC_{25} values ranged from 6.86 to 30.19 mS m^{-1}, while the field capacity survey ranged from 4.23 to 40.28 mS m^{-1}) indicating the EC_{25} still reflects changes in water content and is therefore still viable for use in determining soil sample locations. The mean values for the EC_{25} high site surveys were 28.66 mS m^{-1}, 29.35 mS m^{-1} and 6.97 mS m^{-1}. The mean values for the EC_{25} low site were 30.54 mS m^{-1}, 19.92 mS m^{-1} and 11.29 mS m^{-1}. A statistical comparison of means however showed that the mean EC_{25} values were only statistically different between the August 4th, 2016 and January 8th, 2017 survey days with a p-value of 0.035. The p-values when August 4th, 2016 and August 16th, 2016 were compared was 0.51, and when August 16th, 2016 and January 8th, 2017 were compared was 0.89. A t-test given unequal variances showed that the range of values were statistically significant when all three surveys were compared with each other (p-values were all < 0.001). The alpha for all statistical analysis was 0.05.

Figure 2-5: Graph comparing temperature corrected apparent electrical conductivity to coarse fragment percent dry mass. Colors represent field capacity (blue), below field capacity (light blue), and dry (green) soil conditions. Circles and squares represent sampling locations in high and low corrected neutron count areas, respectively.

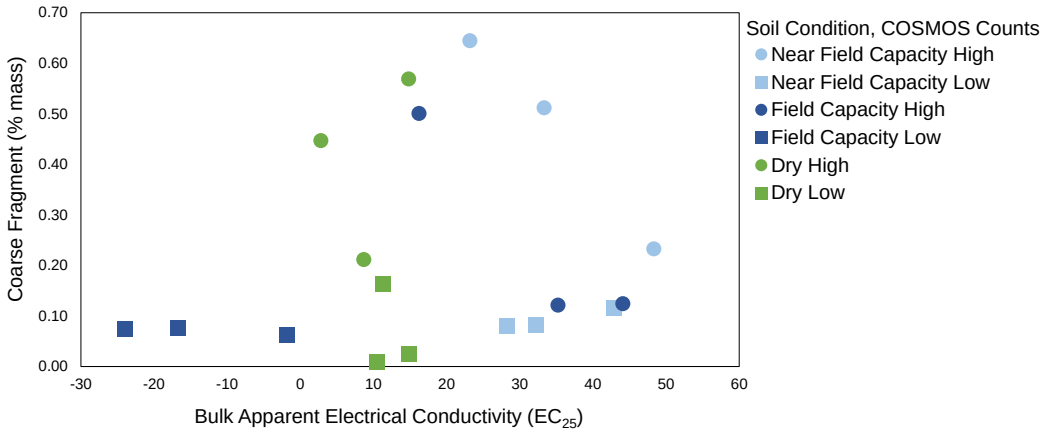

Figure 2-6: Graph comparing temperature corrected apparent electrical conductivity to coarse fragment percent volume. Colors represent field capacity (blue), below field capacity (light blue), and dry (green) soil conditions. Circles and squares represent sampling locations in high and low corrected neutron count areas, respectively.

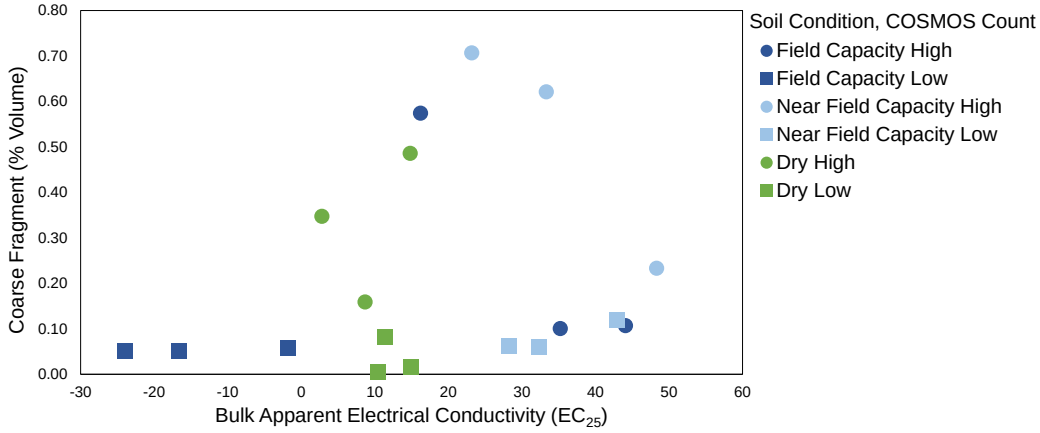

2.3.3 COSMOS Rover Surveys

The three COSMOS high neutron count sites were found on the loamy skeletal association while the lower neutron counts were found on the clay loam soil, as seen in figures Figure 2-7 to 2-9.

Figure 2-7: Map of COSMOS corrected neutron count survey taken on August 4th, 2016. The survey was completed 72 hours after a moderate rainfall event. The ranch received less than 25 mm of rainfall and was not considered to be at field capacity for the duration of the survey. Higher neutron counts were found on the shallow, skeletal chianti-boracho-berrend association soil near rock outcrops. The lower neutron counts were found on the marfa clay loam soil. The locations for EMI surveys and soil samples are marked with a red star. Aerial image from Esri World imagery (ESRI, 2012).

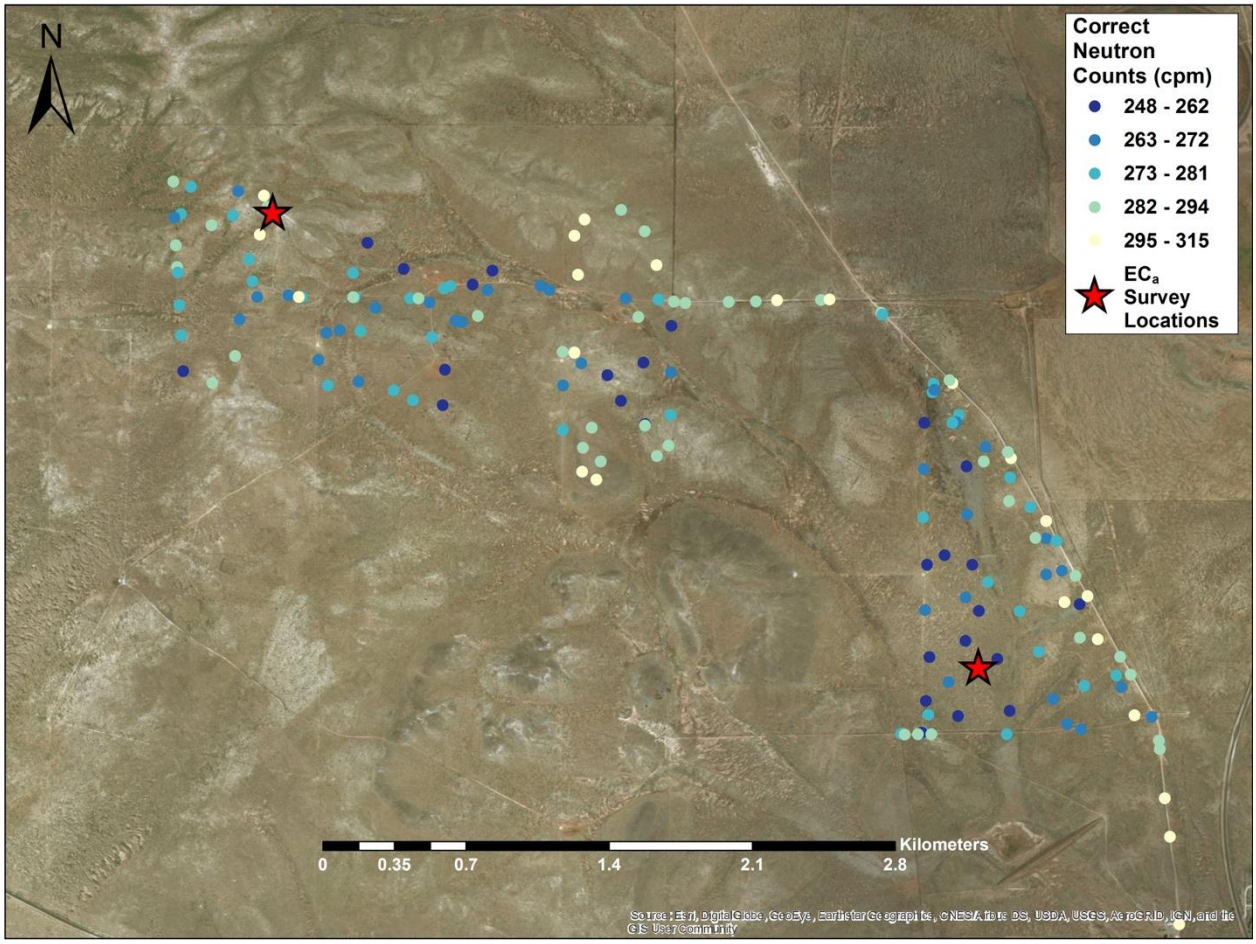

Figure 2-8: Map of COSMOS corrected neutron count survey taken on August 16th, 2016. Prior to the survey, the ranch received three consecutive days of heavy rain. The soil was considered to be at field capacity for the duration of the survey, which began within 24 hours' post rainfall. The locations for EMI surveys and soil samples are marked with a red star. Aerial image from Esri World imagery (ESRI, 2012).

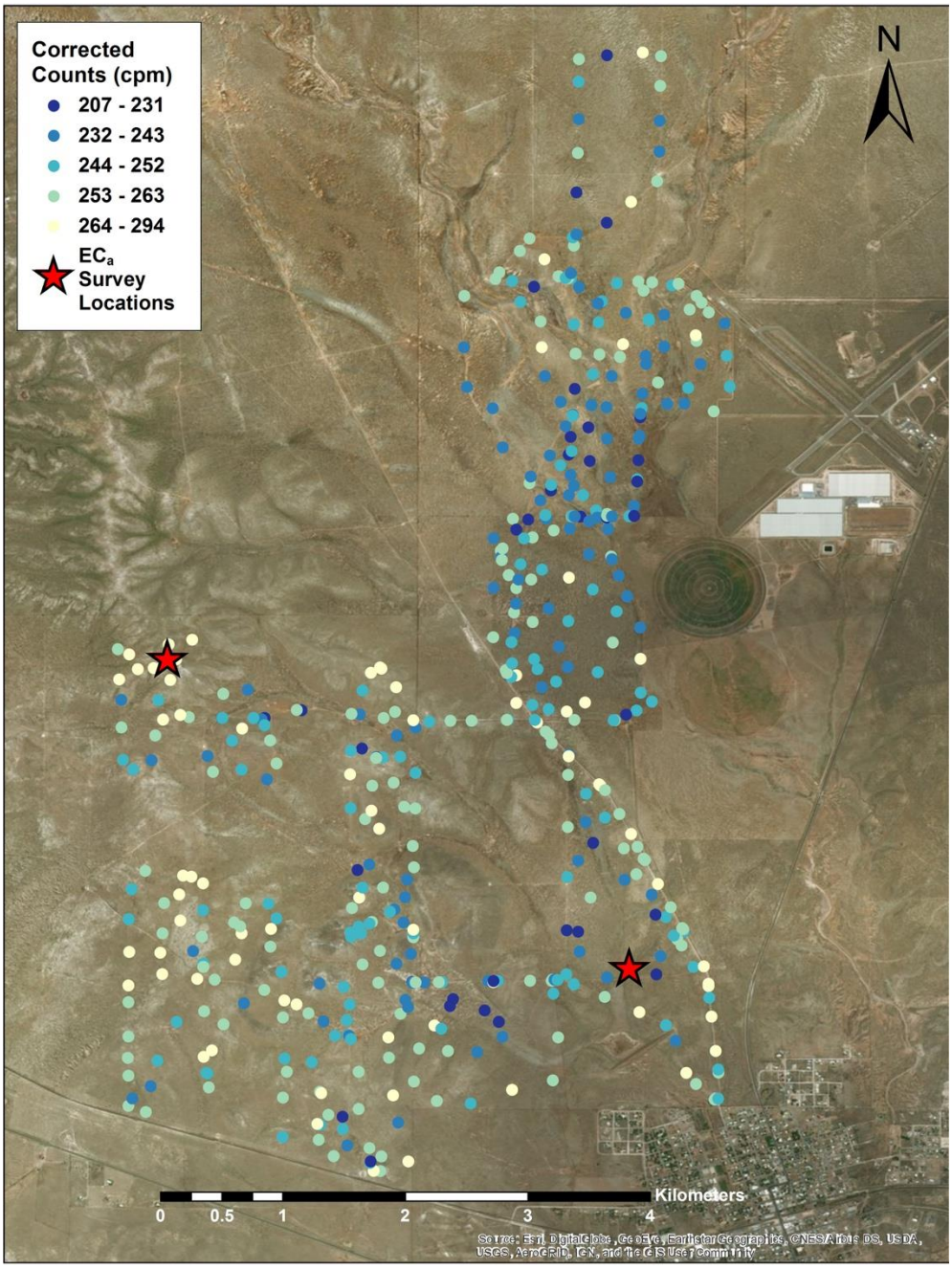

Figure 2-9: Map of COSMOS corrected neutron count survey taken on January 7th, 2016. The last major rainfall event at the ranch occurred in early November of the previous calendar year. The soil was considered to be at its driest soil water content conditions. The locations for EMI surveys and soil samples are marked with a red star. Aerial image from Esri World imagery (ESRI, 2012).

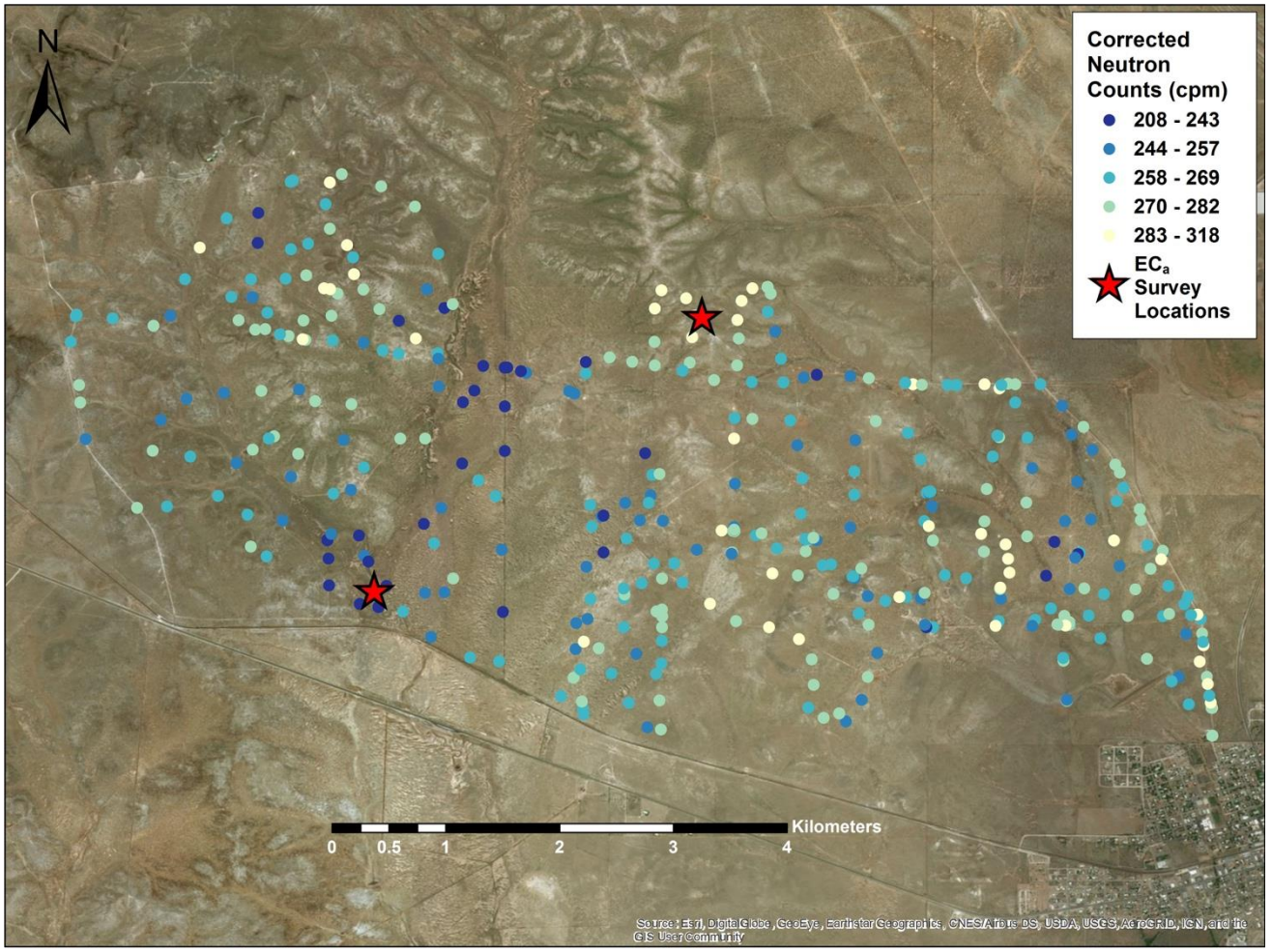

Figure 2-8 shows the COSMOS survey map taken from the field capacity field expedition. Higher neutron counts were consistently found on higher elevation areas, (around 1600 m above sea level) that were the top of hillslopes or rock outcrops, where surface coarse fragments were easily visible. The depth to cemented calcic material on the skeletal soils is mapped between 31 and 53 cm, and depth to bedrock is mapped between 53 and 119 cm (Soil Survey Staff, 2013). The shallow depth to the petrocalcic horizon was observed when collecting our soil bucket samples, where coarse fragments were consistently abundant from the surface to the 30 cm depth for each bucket sample. Areas with the lowest neutron counts were found on the deeper clay loam soil where little to no coarse fragments were observed on both the surface and in the subsurface. There was also a substantial increase in grass vegetation. Neutron counts were within similar ranges between each COSMOS survey; however, overall neutron count decreased in wet conditions. The lowest neutron counts were found on the August 16th survey, when the soil was closest to field capacity. Corrected neutron counts ranged from 248.4 to 300.9 for the below field capacity survey, 223 to 264 for the field capacity survey, and 251 to 289.6 for the dry survey (Figure 2-10).

Figure 2-10: Histograms of corrected neutron count distribution at high and low COSMOS locations for the three survey days.

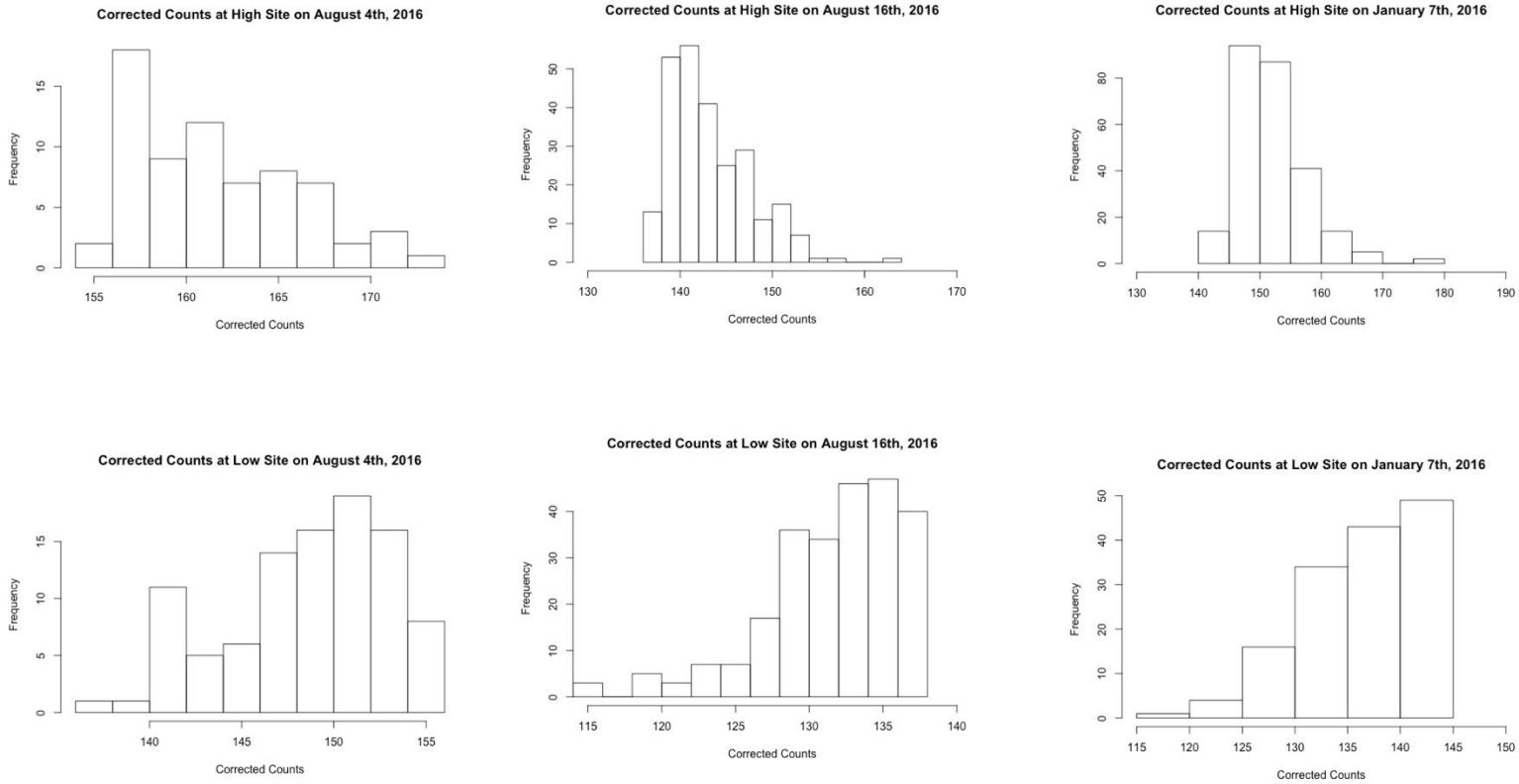

2.3.4 Spatial Interpolation and Calibration of COSMOS Estimations

The assumptions made for this project were: 1) the EM38-MK2 responds to changes in coarse fragment distribution and 2) there is a direct relationship between EC_{25} and soil water content. Based on these assumptions, the EC_{25} values were assumed to respond to both changes in water content and coarse fragment volume. Figure 2-11 shows the spatial interpolated map of the clustered water contents within the COSMOS footprint. The percentage of each cluster and the distance from the COSMOS rover were used to determine the spatial mean water content within the footprint. Once the spatially-weighted mean water content was calculated, the weighted mean water contents were compared to the COSMOS measured water contents (Figure 2-12).

Figure 2-11: Ordinary Kriging map of clustered electrical conductivity values on August 16th, 2016. The three clusters were each assigned a water content measured from bulk soil samples. Each interpolated map was used to calculate soil water content within the COSMOS footprint.

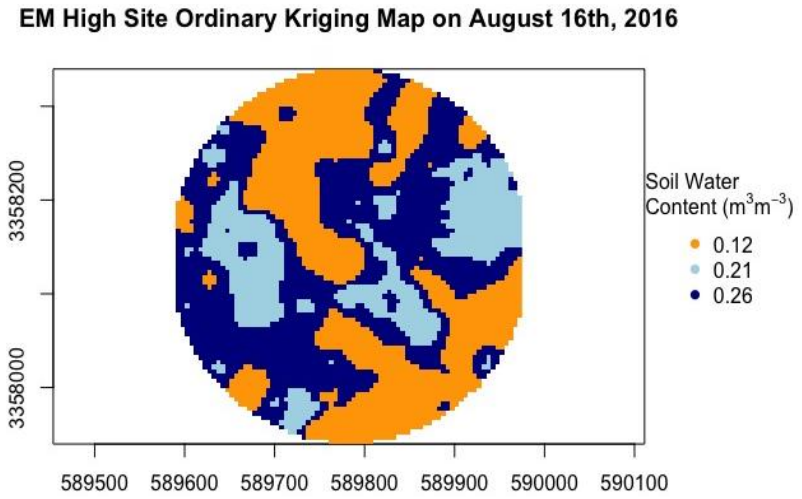

Figure 2-12: Graph comparing COSMOS estimated water content to ground measured water content. The black triangles are spatially-weighted means for each COSMOS calibration site. Colors represent field capacity (blue), below field capacity (light blue), and dry (green) soil conditions. Circles and squares represent sampling locations in high and low corrected neutron count areas, respectively.

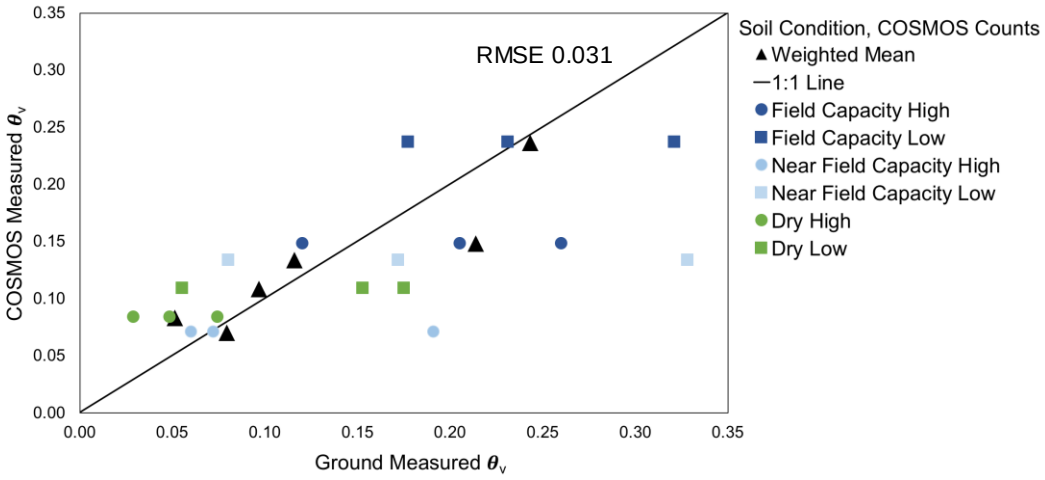

The COSMOS measured water contents increase as the ground-measured water contents increased. Both the COSMOS and ground measured water contents also match the overall wetness conditions for each survey (e.g. higher water contents were estimated on the wettest survey, while the lowest water contents were estimated on the driest survey). Based on these results, COSMOS appears to estimate soil water content at this location with a root mean square error, a measurement of the difference between model estimated and actually observed values, of 0.031.

2.4 Discussion

Previous literature has shown that as water content increases, the bulk apparent electrical conductivity of the soil also increases (Friedman, 2005), indicating a linear relationship between soil water content and EC_a. Water content decreases with an increase in rock fragment volume (Baetens et al., 2009; Cousin et al., 2003; Poesen and Bunte, 1996). Based on these findings, we expected to see a negative linear relationship between coarse fragment volume and electrical conductivity. On survey locations where there is large variability in coarse fragment distribution, the relationship between EC_{25} values and coarse fragments appears to show the expected relationship (Figure 2-5 and 2-6). However, for surveys where there is less coarse fragment variability between soil samples, there does not appear to be a strong correlation between EC_{25} and coarse fragment volume. This could be due to several factors. The most likely factor is that because there is small water content variability, the electrical conductivity values are being influenced by more than one soil property. Doolittle et al. (2014) found lower predictive accuracies when the measured soil property displays low variability. The

second factor is the resistivity of the rocks. Doolittle et al. (2013) found that transect readings over surface rock fragments showed erratic fluctuations. This is due to the fact the resistivity of the rocks prevents the eddy currents from creating the secondary magnetic field used to measure electrical conductivity. The lithology of the rocks is also a possible explanation. The shallow depth to calcic horizons, which has been known to affect EC_a (Brevik and Fenton, 2002), may have influenced the measured readings as well as the potential water holding capacity of the rocks. Further work can quantify the amount of water holding potential the coarse fragments have.

Figure 2-13 shows the relationship between corrected neutron counts and coarse fragment volume. The graph shows that although neutron counts increases with increasing coarse fragment volume, the relationship is not linear. This was particularly interesting, as we expected to see a more direct relationship between neutron counts and coarse fragment volume because of the strong relationship they both have to water content. Previous literature has stated that in order to fully understand the influence coarse fragments have on soil available water, total bulk density, coarse fragment content, water contents for both driest and wettest season conditions, rock fragment particle density, and rock fragment porosity need to be known (Flint and Childs, 1984). For our particular study, rock particle density and porosity were not fully evaluated in regard to their influence on soil available water. Of these, rock fragment porosity should be further investigated, as this physical property could have influenced the volume displacement method used to measure coarse fragment volume.

Figure 2-13: Graph comparing COSMOS corrected neutron counts to the coarse fragment percent volume. The black triangles are spatially-weighted means for each COSMOS calibration site. Colors represent field capacity (blue), below field capacity (light blue), and dry (green) soil conditions. Circles and squares represent sampling locations in high and low corrected neutron count areas, respectively.

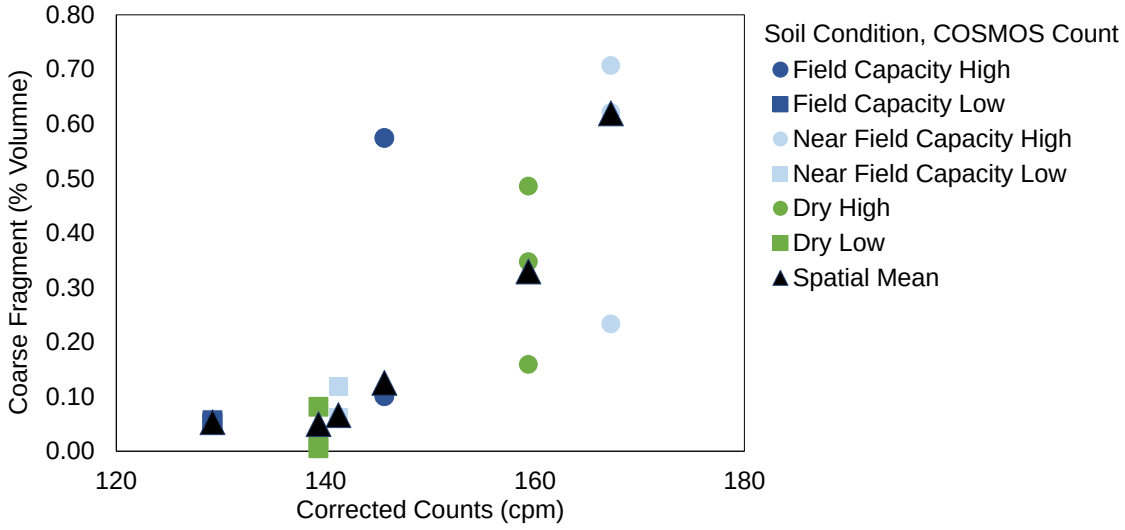

As stated previously, changes in spatial and temporal variation of neutron intensity are corrected for in the cosmos correction factors. However, the correction for geomagnetic latitude references one elevation. To determine if our elevation variation had any effect on neutron counts, we calculated water contents using two different geomagnetic latitude correction factors. The first factor was calculated using the reference elevation at the ranch headquarters. The second calculation allowed the scaling factor to change with elevation. The corrected counts for both calculations were compared by running a simple t-test and regression. The t-test results showed the two different calculations were not statistically different with a p-value of 0.96. Figure 2-14 shows the regression line between the corrected neutron counts when scaling factor was

fixed and allowed to change. The R^2 on the line was 0.98. Although there was no statistical difference between the corrected neutron counts based on the different scaling factor calculations, the root mean square error between the ground measured and COSMOS estimated water contents did increase from 0.031 when the scaling factor changed with elevation to 0.040 when the scaling factor was fixed. Further research should investigate if the scaling factor should always be allowed to change when there is a wide range in elevation.

Figure 2-14: Graph comparing corrected neutron counts when the scaling factor was fixed for one reference elevation versus when the scaling factor changed with elevation.

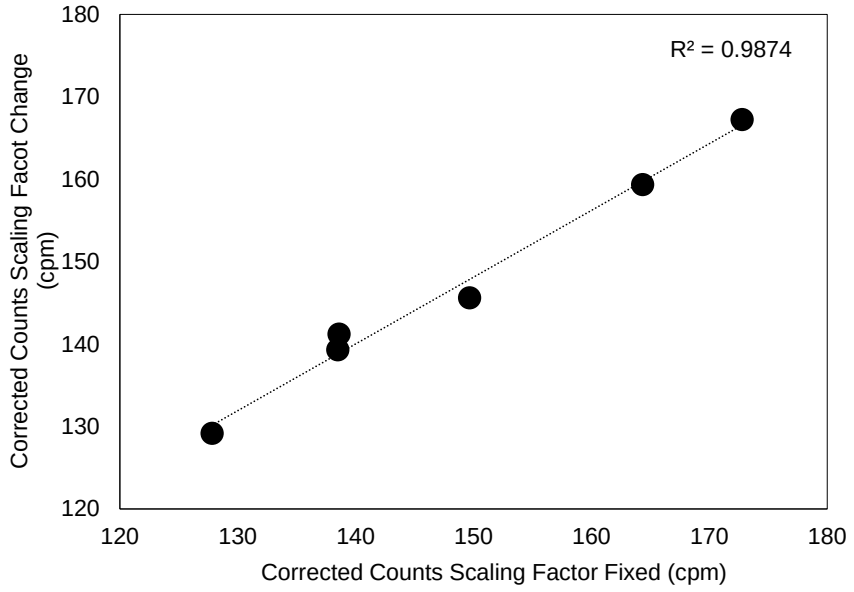

The COSMOS calibration equation can include both a biomass index and soil organic carbon concentration with a correction factor for both. For this study, the vegetation on the ranch was negligible and therefore was not included in the calibration. The amount of soil organic carbon was not known during the time of this study. Future work should quantify the biomass index and soil organic factors to determine if they improve the COSMOS soil moisture measurements.

The increase in coarse fragment percent by volume at the higher hillslopes are consistent with the current understanding of the landscape. Although the focus of this study was on the accuracy of soil moisture readings compared to the number of coarse fragments in the soil, it is important to note the different soil properties associated with the two soil types in question. Further research should consider other hydraulic properties associated with each soil type, to understand their relationship to the distribution of coarse fragments and COSMOS neutron counts.

As a final assessment of the COSMOS rover accuracy, ordinary kriging was performed, and soil moisture maps were created for the majority of the Mimms Ranch. These maps were then compared to another large-scale soil moisture sensor, the Soil Moisture Active Passive mission remote sensing satellite. Soil moisture maps within 24 hours from each survey day were created and compared to the COSMOS maps. Figure 2-15 shows the two different maps for both the wettest and driest survey conditions. The dark blue-green areas of the COSMOS map correspond to the deeper clay loam soil at lower elevations, while the red are higher elevation areas near rock outcrops. It is clear that the SMAP coarse resolution (9000 m scale) is unable to distinguish landscape scale

changes in water content across the ranch. The average water content by pixel under the driest soil conditions was 12.2% for SMAP and 13.3% for COSMOS, while the wettest soil condition water contents were 12.7% for SMAP and 16.8% for COSMOS. Though these values fall within the 4% error for both COSMOS and SMAP, the difference between average pixel values could mean that either sensor is under or overestimating water content. Most likely this is an underestimation from SMAP, as the COSMOS water contents appear to be closely related to the ground measured water contents. This comparison leads us to conclude that COSMOS is accurately mapping soil moisture patterns across the ranch.

Figure 2-15: COSMOS ordinary kriging maps compared to SMAP soil moisture maps on wettest and driest survey days. SMAP maps adapted from SMAP satellite data (O'Neill et al., 2016).

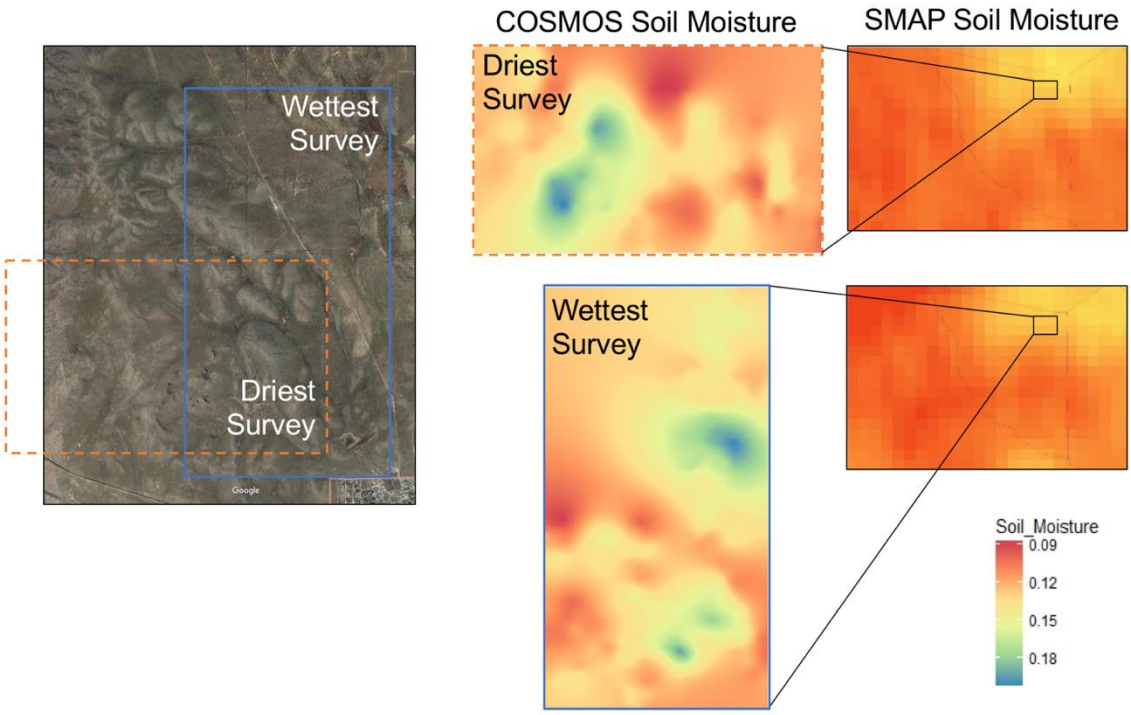

2.5 Summary

The agreement between the preliminary visual observations on the ranch, the relationship between coarse fragment volume and COSMOS corrected neutron counts, and the comparison between the COSMOS estimated and ground measured water contents indicate the strength of the results. The COSMOS rover water content estimations appear to be accurately mapping the spatial variability of the soil moisture on the ranch, even with the scarce sample size (RMSE of 0.031). However, as with larger scale sensors, there is a loss of variability with increasing scale. This was seen with our individual soil samples, where the relationships between water content, electrical conductivity and coarse fragments were not consistently observed at the COSMOS intermediate scale. This is also shown in the map comparison between the COSMOS and SMAP, where the COSMOS displayed more spatial variability in soil moisture than its larger scale counterpart.

Understanding the relationship between soil-water dynamics in skeletal soils is integral for both agricultural and ecological applications at the landscape scale. The COSMOS rover has attractive features that can be used to accomplish this; it is an intermediate scale soil moisture sensor that can take landscape scale measurements quickly and non-invasively and is not dependent on a radioactive source. On the dryland skeletal soils on the Mimms Unit Ranch, the COSMOS rover has now been shown to accurately measure soil moisture patterns needed to make informed management decisions and parameter inputs. Although large scale SMAP maps measure the overall average water content of the ranch, this may not be useful when making inferences at the

landscape scale. For understanding soil moisture patterns in extreme landscapes such as karst savannahs and rangelands with skeletal soils, the COSMOS rover has a promising future for soil moisture mapping.

CHAPTER III

CONCLUSIONS

Intermediate scale surface soil moisture maps and sensors can be necessary tools for landowners, communities and research. These maps can be particularly useful when making efficient land management decisions for urban planning and determining grazing rotations for ranches with limited water resources. Intermediate scale sensors can help protect and monitor natural resources such as groundwater recharge zones, and aid in calculating thresholds for vulnerable soils, such as drylands. Another potential intermediate scale sensors have is their ability to up-scale and down-scale between other soil moisture sensors.

The purpose of this study was to assess the accuracy of a COSMOS rover in estimating soil volumetric water content in a Texas skeletal soil. Some assumptions were made in order to build our methodology. The first was that electrical conductivity has a direct relationship to water content in these soils (when water content increases, so does the electrical conductivity). The second assumption was that there is a linear relationship between coarse fragments and water content. As the volume of coarse fragments in the soil increases, the amount of soil water decreases. The third and final assumption was that there is a linear relationship between coarse fragment volume and electrical conductivity. Based on these assumptions, we collected data at three different spatial scales: 1) COSMOS rover neutron count surveys at the 100-m scale, 2) electrical conductivity surveys at the 10-m scale, and 3) soil samples at the 1-m scale. The

electrical conductivity survey was taken to determine the spatial variability of coarse fragments within the COSMOS footprint.

The relationship between coarse fragment and electrical conductivity was not consistently observed throughout the data. This has been observed in previous literature in the presence of surface fragments or shallow depth to bedrock. It is believed that the strong resistivity of the rocks themselves interfere with the secondary magnetic field of the sensor. Overall electrical conductivity did respond to changes in overall moisture condition. The EM38-MK2 may not be able to quantify rock content in the soil, its variability can still be used to map changes in rock content when a direct relationship between rock fragments and water content exists. Despite the lack of relationship between coarse fragment and electrical conductivity, we did see a response to coarse fragment volume in the corrected neutron counts. This further strengthens the assumption that water content is directly related to rock content at this site.

The biggest limitation of the study was the sample size for ground measured water content. For each COSMOS survey, there were two electrical conductivity surveys, and within each electrical conductivity survey there were three soil samples. The COSMOS was therefore only calibrated with eighteen ground measured samples. Although the COSMOS estimations compare well to the ground measured spatial mean calculated, the results are limited by the assumption that the three ground samples taken within each COSMOS footprint are accurately representative of the water content within the area. Obtaining any more ground-truth samples was unfeasible because of the distance from the research laboratory to the ranch and the sample size needed to meet ASTM standards

based on coarse fragment size. Although the relationship between COSMOS and the ground-measured water contents had an RMSE of 0.031, we were unable to confidently conclude that the COSMOS estimations were fully representative of the spatial variability on the ranch.

Another limitation in the study is the lack of investigation onto the weighted depth of each sensor in question. All three sensors, the COSMOS Rover, EM38-MK2, and SMAP satellite have different measurement depths associated with different moisture conditions. Although the EM38-MK2 and COSMOS rover were assumed to measure within the same depth due to the soil characteristics at the research location, no quantifiable method was done to determine the accuracy of this. Likewise, the measurement depth of the SMAP satellite is the top 5cm of the soil. Although the COSMOS measurement depth depends on the soil moisture condition, it is reading anywhere between the 0-30cm of the soil. No weight was given to the depth of the COSMOS measurement and future research should look into the quantifying the measurement depth of the COSMOS at the research site.

Digital soil mapping is the current method for predicting soil properties in unmeasured locations. Current digital soil maps are limited by the sensor input's volume and error associated with the sampling method. The COSMOS rover has the potential to improve digital soil maps by bridging the gap between large (SMAP) and small (Theta Probe) scale sensor inputs for models and having the ability to measure noninvasively in previously unmeasured locations. Recommendations for future work are to continue to validate SMAP soil moisture maps with COSMOS soil moisture measurements and to

look into using COSMOS estimations to predict other soil properties that are closely related to soil water content.

REFERENCES

Amato, M., B. Basso, G. Celano, G. Bitella, G. Morelli, and R. Rossi. 2008. In situ detection of tree root distribution and biomass by multi-electrode resistivity imaging. Tree Physiol. 28(10):1441-1448. doi: https://doi.org/10.1093/treephys/28.10.1441

ASTM D4700-15. 2015. Standard guide for soil sampling from the vadose zone, ASTM International, West Conshohocken, PA. https://doi.org/10.1520/D4700-15

Beibei Z., M. S. Ming'an, and S. Hongbo. 2009. Effects of rock fragments on water movement and solute transport in a loess plateau soil. Comptes Rendus Geoscience. 341(6):462-472. doi: http://dx.doi.org/10.1016/j.crte.2009.03.009

Boettinger, J.L., A. Moore, S. Keinast-Brown, D. Howell, and A. Hartemink. 2010. Current state of digital mapping and what is next. In: J.L. Boettinger et al., editors, Digital soil mapping: bridging research, environmental application, and operation. Springer Science + Business, Media B.V. New York. 3-4. doi:10-1007/978-90-481-8863-5

Brady, N. C., and R. Weil. 2002. Soil texture (size distribution of soil particles). In: Daryl Fox, editor, The nature and properties of soils. Pearson Education, Ltd. Essex, England. p. 152-157

Brevik, E.C., and T.E. Fenton. 2002. Influence of soil water content, clay, temperature, and carbonate minerals on electrical conductivity readings taken with an EM-38. Soil Horizons. 43(1): 9-13

Chow, T.L., H.W. Rees, J.O. Monteith, P. Toner, and J. Lavoie. 2007. Effects of coarse fragment content on soil physical properties, soil erosion and potato production. Can J Soil Sci 87(5): 565–577. doi: 10.4141/cjss07006

Collow, T.W., and A. Robock, J. Basara, and B. Ilston. 2012. Evaluation of SMOS retrievals of soil moisture over the central United States with currently available in situ observations. J of Geophysical Res. 117(D9): 113. doi:10.1029/2011JD017095

Cousin, I., B. Nicoullaud, and C. Coutadeur. 2003. Influence of rock fragments on the water retention and water percolation in a calcareous soil. Catena 53(2): 97–114. doi: 10.1016/S0341-8162(03)00037-7

Dabas, M. and A. Tabbagh. 2003. A comparison of EMI and DC methods used in soil mapping–theoretical considerations for precision agriculture. In: J. Stafford and

A. Werner, editors, Precision Agriculture. Wageningen Academic Publishers. The Netherlands. 121-127. doi: 10.3920/978-90-8686-514-7

Desilets, D., and M. Zreda. 2003. Spatial and temporal distribution of secondary cosmic-ray nucleon intensities and applications to in situ cosmogenic dating. Earth Planet Sc Lett 206(1-2): 21–42

Desilets, D., Zreda, M. and Prabu, T., 2006. Extended scaling factors for in situ cosmogenic nuclides: new measurements at low latitude. Earth and Planetary Science Letters, 246(3-4), pp.265-276

Desilets, D., M. Zreda, and T. Ferré. 2010. Nature's neutron probe: land surface hydrology at an elusive scale with cosmic rays. Water Resour Res. 46(11): n/a-n/a. doi:10.1029/2009WR008726

Dong, J., T. Ochsner, M. Zreda, M. Cosh, and C. Zou. 2014. Calibration and Validation of the COSMOS Rover for Surface Soil Moisture Measurement. Vadose Zone J 13(4): 0. doi: 10.2136/vzj2013.08.0148

Doolittle, J., M. Petersen, and T. Wheeler. 2001. Comparison of two electromagnetic induction tools in salinity appraisals. J of Soil and Water Conservation. 56(3):257-262

Doolittle, J., J. Chibirka, E. Muñiz, and R. Shaw. 2013. Using EMI and P-XRF to characterize the magnetic properties and the concentration of metals in soils formed over different lithologies. Soil Horizons 54(3): 0

Esri. "World Imagery" [basemap]. Scale not given. "World Imagery Map". February 18, 2012. Accessed February, 2018. www.arcgis.com/home/item.html?id=86de95d4e0244cba80f0fa2c94037b2 .

FAO. 2006. Guidelines for soil description. Rome, 109 pp.

Flint, A.L., and S. Childs. 1984. Phyiscal properties of rock fragments and their effect on available water in skeletal soils. In Soil Science Society of America.

Franz, T., Zreda, Ferre, Rosolem, Zweck, Stillman, Zeng, and Shuttleworth. 2012a. Measurement depth of the cosmic ray soil moisture probe affected by hydrogen from various sources. Water Resour Res 48(8): n/a–n/a.

Franz, T., M. Zreda, R. Rosolem, T. Ferre. 2012b. Field validation of a cosmic-ray neutron sensor using a distributed sensor network. VZJ. 11(4): 0. doi: 0.2136/vzj2012.0046

Franz, T., M. Zreda, R. Rosolem, and T. Ferre. 2013. A universal calibration function for determination of soil moisture with cosmic-ray neutrons. Hydrol Earth Syst Sc 17(2): 453–460. doi: 10.5194/hess-17-453-2013

Han, X., H.J. Franssen, M. Bello, R. Rosolem, H. Bogena, F. Alzamora, et al. 2016. Simultaneous soil moisture and properties estimation for a drip irrigated field by assimilating cosmic-ray neutron intensity. J Hydrol 539: 611–624. doi: 10.1016/j.jhydrol.2016.05.050

Jana, R., A. Ershadi, and M. McCabe. 2016. Examining the relationship between intermediate-scale soil moisture and terrestrial evaporation within a semi-arid grassland. Hydrol Earth Syst Sc 20(10): 3987–4004. doi: 10.5194/hess-20-3987-2016

Jiang, Z., Y. Lian, and X. Qin. 2014. Rocky desertification in southwest china: impacts, causes, and restoration: a review. Earth-Science Reviews. 132:1-2. doi: 10.1016/j.earscirev.2014.01.005

Johnson, P., K. Mayrand, and M. Paquin. 2006. United nations convention to combat global desertification in global sustainable development governance. In: P. Johnson et al., editors, Governing global desertification: linking environmental degradation, poverty, and participation. Ashgate Publishing Co. Burlington, VA. 1-9

Kędzior, M., and J. Zawadzki. 2016. Comparative study of soil moisture estimations from SMOS satellite mission, GLDAS database, and cosmic-ray neutrons measurements at COSMOS station in Eastern Poland. Geoderma 283: 21–31. doi: 10.1016/j.geoderma.2016.07.023

Kim, S., Y.Y. Liu, F. Johnson, R. Parinussa, and A. Sharma. 2015. A global comparison of alternate AMSR2 soil moisture products: Why do they differ? Remote Sens Environ 161: 43–62. doi: 10.1016/j.rse.2015.02.002

McBratney, A., M. Santos, and B. Minasny. 2003. On digital soil mapping. Geoderma 117(1-2): 3–52. doi: 10.1016/s0016-7061(03)00223-4

McNeill, J.D. 1980. Electromagnetic terrain conductivity measurement at low induction numbers. Technical note TN-6. Geonics Limited, Ontario Canada L5T 1CS

Millennium Ecosystem Assessment. 2005. Ecosystems and human well-being: desertification Synthesis. World Resources Institute, Washington, DC. ISBN: 1-56973-590-5

Miller, F. T., R. L. Guthrie 1984. Classification and Distribution of Soils Containing Rock Fragments in the United States1. In: J. D. Nichols, P. L. Brown, W. J.

Grant, editors, Erosion and Productivity of Soils Containing Rock Fragments, SSSA Spec. Publ. 13. SSSA, Madison, WI. p. 1-6. doi:10.2136/sssaspecpub13.c1

O'Neill, P. E., S. Chan, E. G. Njoku, T. Jackson, and R. Bindlish. 2016. SMAP Enhanced L3 Radiometer Global Daily 9 km EASE-Grid Soil Moisture, Version 1. [Soil Moisture]. Boulder, Colorado USA. NASA National Snow and Ice Data Center Distributed Active Archive Center. doi: https://doi.org/10.5067/ZRO7EXJ8O3XI. [Accessed 10/2017].

Palacky, G. J.1987. Clay mapping using electromagnetic induction. First Break 5(8): 295-306. doi: 10.3997/1365-2397.1987015

Pimentel, D., P. Hepperly, J. Hanson, D. Douds, and R. Seidel. 2005. Environmental, energetic, and economic comparisons of organic and conventional farming systems. Bioscience 55(7): 573–582. doi: 10.1641/0006-3568(2005)055[0573:EEAECO]2.0.CO;2

Poesen, J., and Lavee. 1994. Rock fragments in top soils: significance and processes. Catena 23(1): 1–28. doi: 10.1016/0341-8162(94)90050-7

R Core Team (2013). R: A language and environment for statistical computing. R Foundation for Statistical Computing, Vienna, Austria. ISBN 3-900051-07-0, URL: http://www.R-project.org/

Renzullo, L.J., A. Dijk, J. Perraud, D. Collins, B. Henderson, H. Jin, et al. 2014. Continental satellite soil moisture data assimilation improves root-zone moisture analysis for water resources assessment. J Hydrol 519: 2747–2762. doi: 10.1016/j.jhydrol.2014.08.008

Robinson, D., C. Campbell, J. Hopmans, B. Hornbuckle, S. Jones, R. Knight, et al. 2008. Soil moisture measurement for ecological and hydrological watershed-scale observatories: a review. VZJ 7(1): 358. doi: 10.2136/vzj2007.0143

Rosolem R., X. Shuttleworth, M. Zreda, T. Franz, X. Zeng, and S. Kurc. 2013. The effect of atmospheric water vapor on neutron count in the cosmic-ray soil moisture observing system. J Hydrometeorol: 130711124939002.

Rosolem, R., T. Hoar, A. Arellano, J. Anderson, W. Shuttleworth, X. Zeng, and T. Franz. 2014. Translating aboveground cosmic-ray neutron intensity to high-frequency soil moisture profiles at sub-kilometer scale. Hydrology and Earth System Sciences 18(11): 4363–4379. doi: 10.5194/hess-18-4363-2014

Schrön, M., M. Köhli, L. Scheiffele, J. et al., 2017. Improving calibration and validation of cosmic-ray neutron sensors in the light of spatial sensitivity. Hydrol Earth Syst Sc 21(10): 5009–5030.

Samouëlian, A., I. Cousin, A. Tabbagh, A. Bruand, and G. Richard. 2005. Electrical resistivity survey in soil science: a review. Soil Tillage Res 83(2): 173–193. doi: 10.1016/j.still.2004.10.004

Sano, E., A. Huete, D. Troufleau, M. Moran, and A. Vidal. 1998. Relation between ERS-1 synthetic aperture radar data and measurements of surface roughness and moisture content of rocky soils in a semiarid rangeland. Water Resour Res 34(6): 1491–1498. doi: 10.1029/98WR00032

Sheets, K., and J. Hendrickx. 1995. Noninvasive soil water content measurement using electromagnetic induction. Water Resour Res 31(10): 2401–2409. doi: 10.1029/95WR01949

Soil Survey Staff. 2010. Keys to Soil Taxonomy. Washington, DC. In: U.S.D.A.-N.R.C. Service (Ed.), p. 346

Soil Survey Staff. 2016. Soil Series Classification Database. USDA-NRCS https://www.nrcs.usda.gov/wps/portal/nrcs/main/soils/survey/class/. (accessed 26 Sept. 2016)

Soil Survey Staff. 2016. Soil Survey of Presidio County, Texas. http://soils.usda.gov/survey/printed_ surveys/. (accessed 26 Sept. 2016)

Throop, H.L., S.R. Archer, H.C. Monger, and Waltman. 2012. When bulk density methods matter: Implications for estimating soil organic carbon pools in rocky soils. J Arid Environ 77: 66–71. doi: 10.1016/j.jaridenv.2011.08.020

Yair, A. and Shachak, M., 1987. Studies in watershed ecology of an arid area. In: L. Berkofsky and M.G. Wurtele (editors), Progress in Desert Research. Rowman and Littlefield, Totowa, NJ, p. 145-193

Ye, N., J. Walker, D. Ryu, C. Rudiger, and R. Gurney. 2009. The effect of rock cover fraction on the retreival of surface soil moisture at L-band. 18th World IMACS/MODSIM. Congress, Cairns, Australia. July 13-17.

Zhu, X., M. Shao, C. Zeng, X. Jia, L. Huang, Y. Zhang, and J. Zhu. 2016. Application of cosmic-ray neutron sensing to monitor soil water content in an alpine meadow ecosystem on the northern Tibetan Plateau. J Hydrol 536: 247–254. doi: 10.1016/j.jhydrol.2016.02.038

Zreda, M., D. Desilets, T. Ferré, and R. Scott. 2008. Measuring soil moisture content non-invasively at intermediate spatial scale using cosmic-ray neutrons. Geophysical Research Letters 35(21). doi:10.1029/2008GL035655

Zreda, Shuttleworth, Zeng, Zweck, Desilets, Franz, Rosolem, and Ferre. 2012. COSMOS: The COsmic-ray Soil Moisture Observing System. Hydrology Earth Syst Sci Discuss 9(4): 4505–4551.